

Recombinant AAV genome size effect on viral vector production, purification, and thermostability

Nermin Ibreljic,^{1,2} Benjamin E. Draper,³ and Carl W. Lawton¹

¹Department of Chemical Engineering, University of Massachusetts Lowell, One University Avenue, Lowell, MA 01854, USA; ²Sarepta Therapeutics, 55 Blue Sky Drive, Burlington, MA 01803, USA; ³Megadalton Solutions, 3750 E. Bluebird Lane, Bloomington, IN 47401, USA

Adeno-associated virus (AAV) has shown great promise as a viral vector for gene therapy in clinical applications. The present work studied the effect of genome size on AAV production, purification, and thermostability by producing AAV2-GFP using suspension-adapted HEK293 cells via triple transfection using AAV plasmids containing the same GFP transgene with DNA stuffers for variable-size AAV genomes consisting of 1.9, 3.4, and 4.9 kb (ITR to ITR). Production was performed at the small and large shake flask scales and the results showed that the 4.9 kb GFP genome had significantly reduced encapsidation compared to other genomes. The large shake flask productions were purified by AEX chromatography, and the results suggest that the triple transfection condition significantly affects the AEX retention time and resolution between the full and empty capsid peaks. Charge detection-mass spectrometry was performed on all AEX full-capsid peak samples showing a wide distribution of empty, partial, full length, and copackaged DNA in the capsids. The AEX-purified samples were then analyzed by differential scanning fluorimetry, and the results suggest that sample formulation may improve the thermostability of AAV genome ejection melting temperature regardless of the packaged genome content.

INTRODUCTION

According to the US Food and Drug Administration Cellular, Tissue, and Gene Therapies Advisory Committee, adeno-associated virus (AAV) production methods produce not only the therapeutic, full AAV capsid, containing the genome of interest but also product-related impurities consisting of capsids that are mispackaged with truncated genome, residual plasmid, host cell DNA, or empty capsids, containing no DNA at all.¹ Purification methods of AAV consist of anion exchange (AEX) chromatography, which is used to enrich full AAV capsids by separating out empty capsids through exploitation of surface charge differences.² The current theory for charge-based separation is that full AAV capsids have a lower isoelectric point (pI ~5.9) than the empty AAV capsids (pI ~6.3) induced by the presence of the negatively charged DNA packaged inside.^{3,4} AEX chromatography methods have been developed at both analytical and preparative scales for optimized full-capsid enrichment across multiple AAV serotypes by evaluating multiple salts, buffer excipients, pH conditions, and elution schemes.^{3,5-7} An AEX high-performance liquid chromatography method achieving baseline

separation of full and empty capsids across AAV6 samples with unique genomes of different sizes ranging from 2.5 to 5.2 kb has shown similar retention times across all of the samples tested (< 5% relative SD), indicating that the method performance was independent of the size of the encapsidated genome.⁶

It is not well understood what effect that AAV capsid heterogeneity has on the charge-based separation by AEX chromatography. High-resolution native mass spectrometry (MS) with spectral simulations have demonstrated that AAV capsids assemble by random incorporation of viral protein (VP) subunits, resulting in widely heterogeneous capsids with varying VP stoichiometries. Even the most abundant capsid composition represents less than 2.5% of the total capsid population.⁸ Liquid chromatography-MS (LC-MS) analyses have been used to characterize AAV posttranslational modifications (PTMs), revealing a total of 52 PTMs with varying abundance depending on the serotype.⁹ Two-dimensional gel electrophoresis has been used to resolve pIs ranging from pH 6.3 to >7.0 for each VP.¹⁰ Both native and denaturing capillary isoelectric focusing methods for AAV have shown multiple pIs across samples when characterizing charge heterogeneity.^{11,12} The presence of these isoforms suggests that each VP has the potential to undergo multiple charge-altering modifications.

The present work studied the effect of the genome size on AAV production, purification, and thermostability by producing AAV2-GFP using suspension-adapted HEK293 cells via triple transfection with three different sizes of single-stranded AAV genome containing GFP consisting of 1.9, 3.4, and 4.9 kb (inverted terminal repeat [ITR] to ITR). A small-scale custom design of experiments (DoE) was performed on the 125-mL shake flask scale evaluating 15 different transfection conditions for each genome size followed by large shake flask production to be purified by affinity capture chromatography. Three transfection conditions for each of the AAV2-GFP productions were then purified by AEX chromatography to evaluate the effect of the genome size and transfection condition on the charge-based

Received 29 March 2023; accepted 12 January 2024;
<https://doi.org/10.1016/j.omtm.2024.101188>.

Correspondence: Nermin Ibreljic, Department of Chemical Engineering, University of Massachusetts Lowell, One University Avenue, Lowell, MA 01854, USA.

E-mail: nermin_ibreljic@student.uml.edu



separation of the full and empty capsids and the resulting enrichment of full capsids by orthogonal methods. The thermostability of the AEX-purified samples were analyzed by differential scanning fluorimetry (DSF) with SBYR gold dye to determine the genome ejection melting temperature (T_{m1}) and capsid melting temperature (T_{m2}). In this study, genome ejection melting temperature was defined as the maximum absorbance change (dA/dT) in the fluorescence intensity curve.

RESULTS

Oversized GFP genome size decreases viral genome production and encapsidation

Study 1 was a 6 factor, 3 to 4 level custom design DoE of 15 conditions using 125 mL shake flasks, and 30 mL working volume for each of the 3 GFP genomes, for a total of 45 experiments. The DoE tested the viable cell density (VCD) at transfection (2.00E+06, 2.50E+06, 3.00E+06, 4.00E+06 cells/mL); DNA amounts (1.0, 1.5, 2.0 $\mu\text{g}/\text{E}+06$ cells); pRep/Cap:pHelp:pGOI plasmid ratios (1-3:1-3:1-3, which were then normalized relative to the pHelp plasmid ratio, making the ratios 0.33-3.0:1:0.33-3.0), and polyethylenimine (PEI):DNA ratios (0.75, 1.0, 1.25 $\mu\text{g}/\mu\text{g}$) as shown in [Table S1](#). The viral genome (vg) titer results for each GFP genome size (1.9, 3.4, and 4.9 kb) are ordered by transfection condition tested in [Figures S1-S3](#). The average vg titer for GFP genomes 1.9, 3.4, and 4.9 kb are 1.73E+10, 1.47E+10, and 3.73E+09 vg/mL, respectively, and [Figure 1A](#) shows that vg titer production of the 1.9 and 3.4 kb GFP genome sizes are not significantly different from each other ($p < 0.2599$), but are both significantly different from the 4.9 kb genome ($p < 0.0001$).

For study 2, 4 transfection conditions were chosen and scaled up to 3 L shake flask, 1 L working volume for each of the 3 GFP genome sizes and then purified by affinity capture chromatography ([Table S2](#)). Transfection condition 1 was based on the JMP software prediction profiler as the optimal condition based on the results from study 1, transfection condition 2 was the condition 13 from study 1 that had the highest vg titer, transfection condition 3 was the same as transfection condition 1 with the VCD set to 4.00E+06, and transfection condition 4 was the same as transfection condition 5 from study 1. The average purified vg yields for GFP genomes 1.9, 3.4, and 4.9 kb are 6.43E+09, 7.37E+09, and 1.20E+09 vg/mL cell culture, respectively ([Figure S4](#)). The average purified capsid (cp) yields are 2.40E+11, 3.25E+11, and 2.57E+11 cp/mL cell culture, respectively ([Figure S5](#)). The average purified vg/cp ratio (%) for GFP genomes 1.9, 3.4, and 4.9 kb are 3.27%, 2.69%, and 0.75%, respectively ([Figure S6](#)). The results of the purified vg/cp ratio (%) by GFP genome size for study 2 ([Figure 1B](#)) show that the 1.9 and 3.4 kb GFP genome sizes are not significantly different from each other ($p < 0.5133$) but are each significantly different from the 4.9 kb genome ($p < 0.015$ and $p < 0.046$, respectively).

AEX chromatography results

Three of the affinity capture chromatography-purified AAV2-GFP conditions were purified by AEX chromatography using a linear elution gradient ([Table S3](#)). The empty and full peak fractions

were collected based on their A280 and A260 absorbance spectra of the chromatogram and tested for vg and cp titer. The AEX chromatography mass balance results for each transfection condition (1-3) and GFP genome size (1.9, 3.4, and 4.9 kb) are shown in [Tables S4-S9](#), showing high recovery and good orthogonality with the AEX chromatograms shown in [Figure 2](#). The conductivity (mS/cm) and retention time (min) between the full and empty peaks for each AEX experiment were measured based on the maxima of the A280 absorbance signal of the peaks ([Tables S10 and S11](#)). The change in conductivity ($\Delta\text{conductivity}$) and retention time (Δt) and the resolution between peaks (R_s) were calculated to be compared between the GFP genome size and the transfection condition performed ([Table 1](#)). When comparing AEX Δt and R_s results across multiple genome lengths ([Figure S7](#)), the triple transfection condition had a significant impact on the charge-based separation of the full and empty capsid peak ($p = 0.0007$ and $p < 0.0001$, respectively) compared to the GFP genome size ($p = 0.9187$ and 0.9997 , respectively).

AEX purified AAV2-GFP encapsidation results

All of the samples from the AEX experiments were concentrated using a 50-kDa molecular weight cutoff spin filter to perform UV/dynamic light scattering (DLS) and CD-MS quantitation. Each of the full capsid peak samples were submitted for CD-MS to quantify the mass distribution of empty, partial, full, and copackaged genomes. An empty AAV2 sample with the average 5:5:50 composition of VP1:2:3 is calculated to have a mass of approximately 3.75 MDa. The expected mass of each GFP genome is 0.7, 1.19, and 1.68 MDa for the 1.9, 3.4, and 4.9 kb GFP packaged genomes, respectively; thus, the expected mass of a fully packaged AAV2-GFP sample is known and compared to the mass distribution generated by CD-MS. The CD-MS mass histogram results ([Figure 3](#); [Tables S12 and S20](#)), and the charge versus mass scatterplot results ([Figure S8](#)) show a wide distribution of empty, partial, full, and copackaged AAV2 capsids, with the results summarized in [Table 2](#). The samples contained 2%-33% full-length genome, with the 4.9 kb GFP genome productions containing more partial capsids than full capsids. The average capsid aggregation (> 5.60 MDa) was observed to increase between transfection conditions 1, 2, and 3 independent of GFP genome size, with transfection condition 3 containing the most aggregation. Based on the expanded CD-MS mass histogram (0-25 MDa) in [Figure S9](#), the capsid aggregation was primarily attributed to empty capsid dimer because the peak mass averaged 7.5 MDa since an empty AAV2 capsid mass was 3.75 MDa. Aggregate masses indicated negligible aggregation of the DNA-containing capsids. The full capsid ratio (%) results by vg/cp titer ratio, UV/DLS, and CD-MS methods of the AEX full peaks for each experiment are shown in [Table 3](#). The vg/cp full capsid ratio results are likely underreported when compared to the UV/DLS and CD-MS results because the viral genome titer measurement relies on targeting the GFP transgene, which may be missing if there are significant truncations occurring during genome packaging (which CD-MS is showing). The results suggest that triple transfection of AAV2 with the 4.9 kb GFP genome does not efficiently package the complete genome, with all

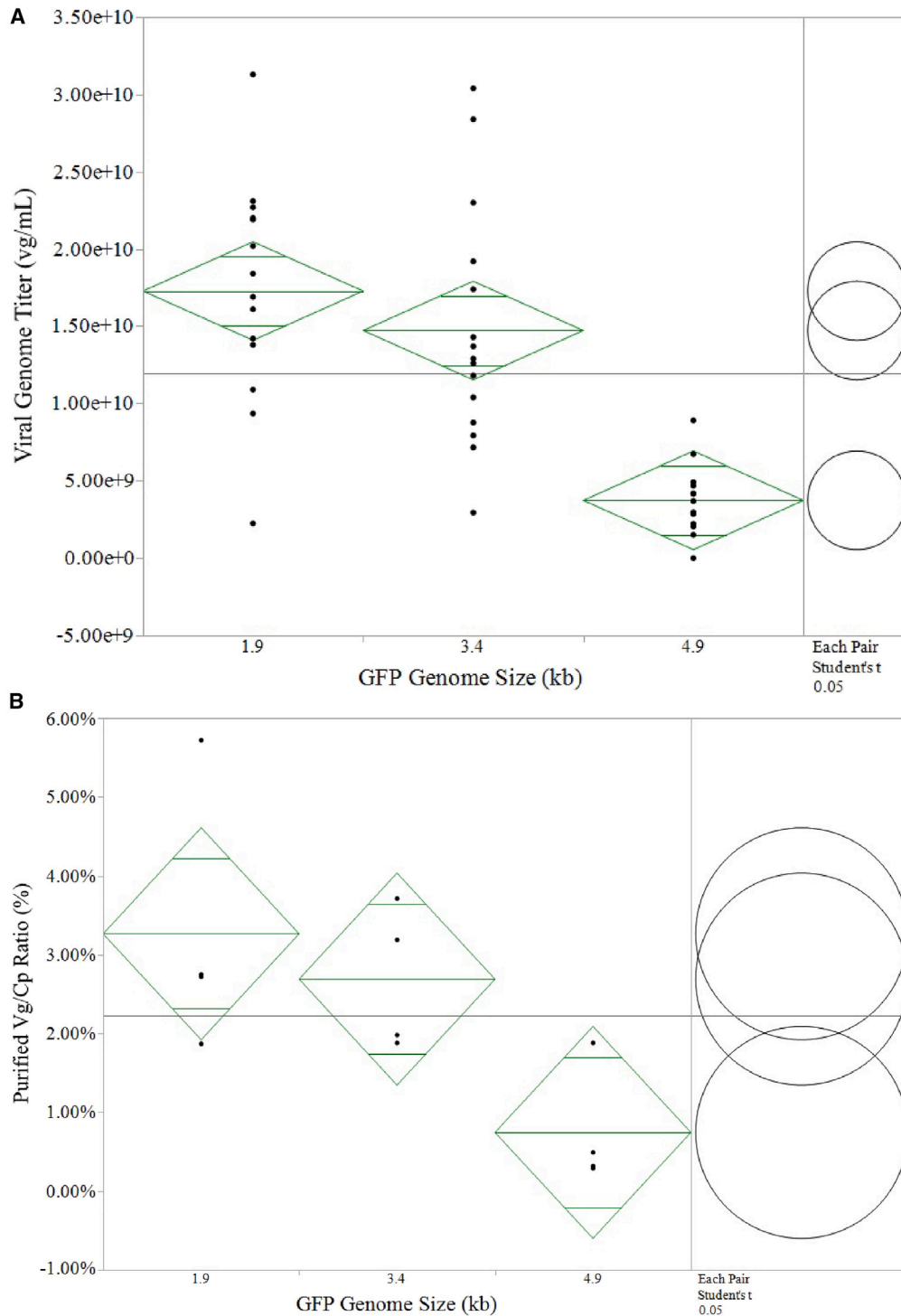


Figure 1. GFP genome size effect on AAV production and encapsidation

(A) One-way means and ANOVA analysis of the viral genome titer (vg/mL) by GFP genome size for study 1. A Student's t test comparing each pair of GFP genome sizes is shown at right. The vg titer production of the 1.9 and 3.4 kb genomes are not significantly different ($p < 0.2599$) but are both significantly different from the 4.9 kb genome ($p < 0.0001$). (B) One-way means and ANOVA analysis of the purified vg/cp ratio (%) by GFP genome size for study 2. A Student's t test comparing each pair of GFP genome sizes at right. The purified vg/cp ratio (%) of the 1.9 and 3.4 kb genomes are not significantly different from each other ($p < 0.5133$) but are each significantly different from the 4.9 kb genome ($p < 0.015$ and $p < 0.046$ respectively).

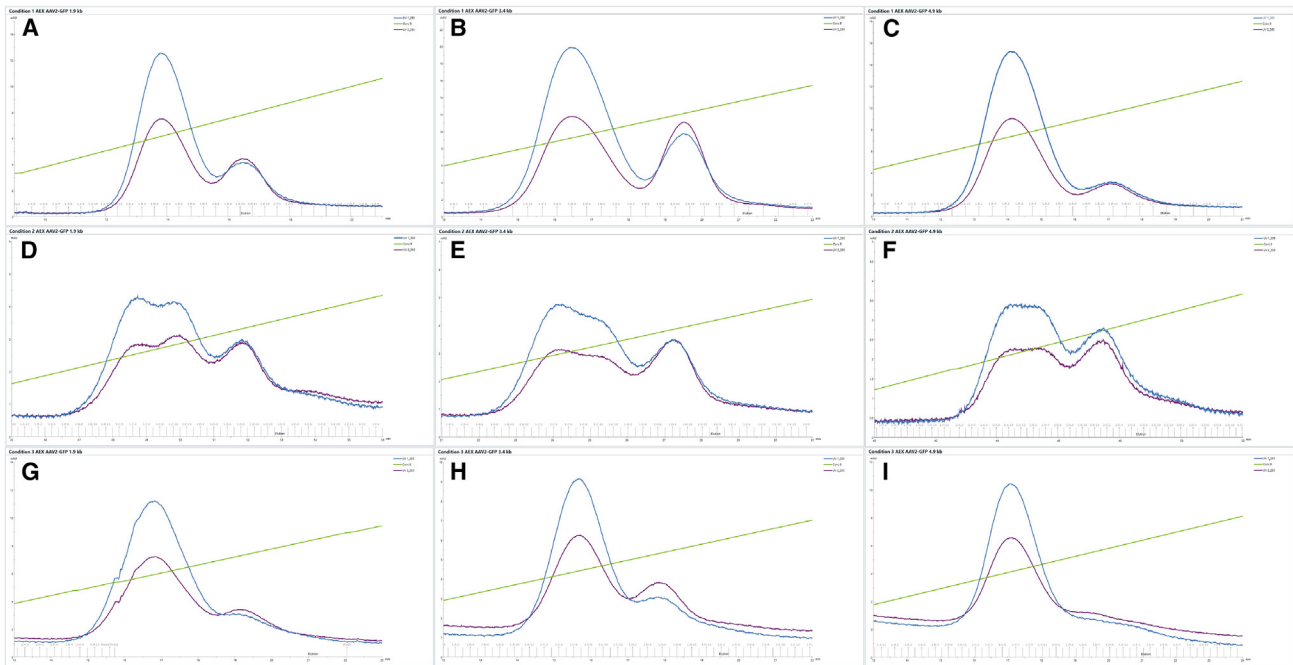


Figure 2. AEX chromatograms of AAV2-GFP purifications

(A) Transfection condition 1 AAV2-GFP 1.9 kb. (B) Transfection condition 1 AAV2-GFP 3.4 kb. (C) Transfection condition 1 AAV2-GFP 4.9 kb. (D) Transfection condition 2 AAV2-GFP 1.9 kb. (E) Transfection condition 2 AAV2-GFP 3.4 kb. (F) Transfection condition 2 AAV2-GFP 4.9 kb. (G) Transfection condition 3 AAV2-GFP 1.9 kb. (H) Transfection condition 3 AAV2-GFP 3.4 kb. (I) Transfection condition 3 AAV2-GFP 4.9 kb.

DNA-containing capsids having masses below that of a full 4.9 kb genome (Figure S10). When evaluating different triple transfection conditions for a single genome size, the AEX Rs trends with the full capsid ratio by the orthogonal methods, but does not trend when comparing different genome lengths with the same transfection condition (Figure S11).

AAV peak CE-SDS-LIF capsid purity vs. transfection condition

The concentrated AAV2-GFP AEX full and empty capsid peak samples were tested by capillary electrophoresis with SDS using laser-induced fluorescence (CE-SDS-LIF) for capsid protein purity (%) as shown in Figure S12, with the results summarized in Tables 4 and S21, respectively. CE-SDS-LIF reports any non-VP1/2/3 peaks as an impurity, which may include low-molecular-weight degraded VP1/2/3 proteins. The results suggest that the AEX empty capsid peak has a higher capsid protein purity than the full capsid peak and that the transfection condition affects the capsid protein purity of the full capsid peak sample (Figure S13).

AAV2-GFP AEX full and empty capsid peak sample thermostability

AAV2-GFP AEX chromatography full and empty capsid peak samples were analyzed by DSF to generate a genome ejection melting curve and static light scattering (SLS) 473 curve for severe aggregation (Figure 4). The average genome ejection melting temperatures ($T_{m1, \text{avg}}$ and $T_{m2, \text{avg}}$) and average aggregation temperature ($T_{\text{agg., avg}}$) are reported

in Tables S22–S26, respectively. The full capsid peak samples had two transition points for genome ejection (Figure 4A), with $T_{m1, \text{avg}}$ being the ejection of the genome because the capsid unfolds before completely unfolding followed by $T_{m2, \text{avg}}$, where the capsid completely unfolds, releasing the remainder of the genome. The $T_{\text{agg., avg}}$ (Figure 4B) closely matches the $T_{m2, \text{avg}}$, because severe aggregation begins once the capsid proteins have completely unfolded, releasing the packaged genome. Since the empty capsid samples had such a low vg titer, the fluorescence intensity decreases over the course of the thermal ramp until the capsid breaks apart, resulting in only one $T_{m, \text{avg}}$ value (Figure 4C). This matches the $T_{\text{agg., avg}}$ value (Figure 4D). The average genome ejection melting temperature of the AAV2 full capsid peak samples tested in this work was $T_{m1, \text{avg}} = 59.16^\circ\text{C} \pm 1.37^\circ\text{C}$. The average capsid melting temperature and average capsid aggregation temperature for all of the AAV2 full capsid peak samples tested in this study were $T_{m2, \text{avg}} = 69.60^\circ\text{C} \pm 0.36^\circ\text{C}$ and $T_{\text{agg., avg}} = 69.23^\circ\text{C} \pm 0.59^\circ\text{C}$; for the empty capsid peak samples, they were $T_{m, \text{avg}} = 71.02^\circ\text{C} \pm 0.88^\circ\text{C}$ and $T_{\text{agg., avg}} = 69.44^\circ\text{C} \pm 0.71^\circ\text{C}$, respectively.

DISCUSSION

The genome packaging limit of AAV capsids has been reported to be ~5.2 kb, and previous literature has observed genome truncations during packaging that increase in abundance as the genome exceeds the capsid packaging limit.^{13–17} The AAV production literature has shown that AAV yields varied depending on the capsid serotype,

Table 1. AEX chromatography Δ Conductivity, Δ t retention time, and Rs results for empty and full capsid peaks

Transfection condition	Genome size, kb	Δ Conductivity peaks, mS/cm	Δ t retention time peaks	Rs peaks
1	1.9	2.24	2.67	0.93
	3.4	2.53	3.05	0.98
	4.9	2.49	2.99	0.93
2	1.9	2.48	1.96	0.54
	3.4	2.52	2.03	0.54
	4.9	2.36	2.05	0.56
3	1.9	1.97	2.39	0.76
	3.4	1.78	2.21	0.72
	4.9	1.99	2.45	0.74

The conductivity measurement (mS/cm) and retention time (min) at the A280 maxima of the AEX chromatography for the AEX empty and full capsid peak and the difference in conductivity (mS/cm), retention time (min), and peak resolution (Rs) calculated.

ITR-ITR configuration (single stranded or self-complementary), triple transfection plasmid ratios, host cell VCD at transfection, total DNA charge, and the ratio of transfection reagent to total DNA.^{18–22} The viral genome production and encapsidation results from this work show that the single-stranded 4.9 kb GFP genome did not efficiently package into AAV2 capsids as shown by the CD-MS profiles (Figure 3) resulting in decreased viral genome production (vg/mL), likely due to packaged genome truncations missing the GFP transgene region being targeted by the PCR method (Figure 1). Previously reported literature on AAV genome packaging capacity used AAV samples prepared by cesium chloride-based ultracentrifugation, which biased the AAV genome sizing results by removing AAV capsids that were less dense than the full capsid band that may have contained truncated genomes, providing insight into the AAV packaging limit but not the AAV packaging efficiency.^{13–17} The AAV2 from this work was purified using affinity capture chromatography followed by AEX chromatography for charge-based separation.

The AEX chromatography results suggest that charge-based separation of full and empty AAV capsids is not in all cases necessarily driven by the packaged genome, but rather is highly driven by upstream production conditions likely due to other product quality attributes (Figure 2). The CD-MS data in this study showed that although the collected full peak from AEX chromatography contains almost all of the viral genome by mass balance calculations (Tables S4–S6), it contains a heterogeneous mixture of predominantly empty capsids, followed by partially packaged, full-length, and co-packaged DNA in the capsids (Figure 3; Table 2). Orthogonal methods for quantifying the relative distribution of AAV encapsidation have been compared in previous literature such as sedimentation velocity analytical ultracentrifugation (sv-AUC), CD-MS, cryoelectron microscopy, titer ratio, size-exclusion chromatography-multiangle light scattering, SEC A260/A280, and UV A260/A280, with sv-AUC and CD-MS described as the gold

standard methods for characterization due to their accuracy and ability to resolve partial genome containing AAV species, respectively, which other methods currently do not.²³ Advances in sv-AUC computational methods have resulted in correlations between the sedimentation coefficient and the packaged genome size.²⁴ One limitation of sv-AUC has been that partial species often get resolved as a single or dual peak, which are calculated as an average density of the species to then be correlated to a packaged genome size. This work relied primarily on CD-MS because this method can quantify the total mass distribution of the AAV sample across 0–25 MDa to show the entire distribution of partial genome-containing AAV capsids and identify the mass of the packaged genome.

The theory for charge-based separation of full and empty AAV capsids has been that full genome-containing AAV capsids have a lower pI than the empty AAV capsids due to the presence of negatively charged DNA packaged inside and that this small difference in surface charge is exploited during AEX chromatography.^{3,4} Accordingly, a new theory is derived for the phenomena of charge-based separation of full and empty AAV capsids that the surface charge differences exploited during AEX chromatography can be a result of different capsid structures generated during AAV production. The AEX Rs between the full and empty peaks is highly driven by the transfection condition across the different genome sizes tested, and increased resolution did not in all of the cases indicate increased encapsidation when comparing the same transfection condition and AAV serotype across different genome sizes (Table 1). The triple transfection condition was shown to affect AAV aggregation (Figures S8 and S9) and capsid protein purity (Table 4) of the AEX full capsid peak across the GFP genome sizes tested. When evaluating different transfection conditions for AAV production, the dynamic binding capacity of the AEX column to the AAV should be reexamined since the charge profile of the heterogeneous AAV pool may shift the AEX chromatography profile.

The transfection condition of the AAV2-GFP samples did not significantly affect the capsid melting temperature ($T_{m, \text{ avg.}}$ or $T_{\text{agg., avg.}}$) as expected based on the previous literature, which has shown that the capsid melting temperature for the same AAV serotype is independent of the sample preparation and presence/lack of packaged genome.²⁵ In the present work, the average genome ejection melting temperature of the full capsid peak samples was $T_{m1, \text{ total avg.}} = 59.16^\circ\text{C} \pm 1.37^\circ\text{C}$, whereas the average capsid melting temperature was $T_{m2, \text{ avg.}} = 69.60^\circ\text{C} \pm 0.36^\circ\text{C}$ and $T_{\text{agg., avg.}} = 69.23^\circ\text{C} \pm 0.59^\circ\text{C}$. The results show a 10°C difference between capsid genome ejection and complete capsid disassembly for AAV2 in this formulation tested. The capsid melting temperatures for both the full and empty capsid peak samples are well aligned with previously reported AAV2 capsid melting temperatures of $T_m = 69.6^\circ\text{C} \pm 0.5^\circ\text{C}$ and $T_m = 68.2^\circ\text{C} \pm 0.6^\circ\text{C}$.^{26,27} The previous literature on AAV2 capsid thermostability has shown that AAV2 is one of the least stable serotypes, with a genome ejection melting temperature $T_{m1} = 49.6^\circ\text{C}$ when using a formulation of PBS with 0.001% Pluronic-F68.²⁸ The $T_{m1, \text{ avg.}}$ of

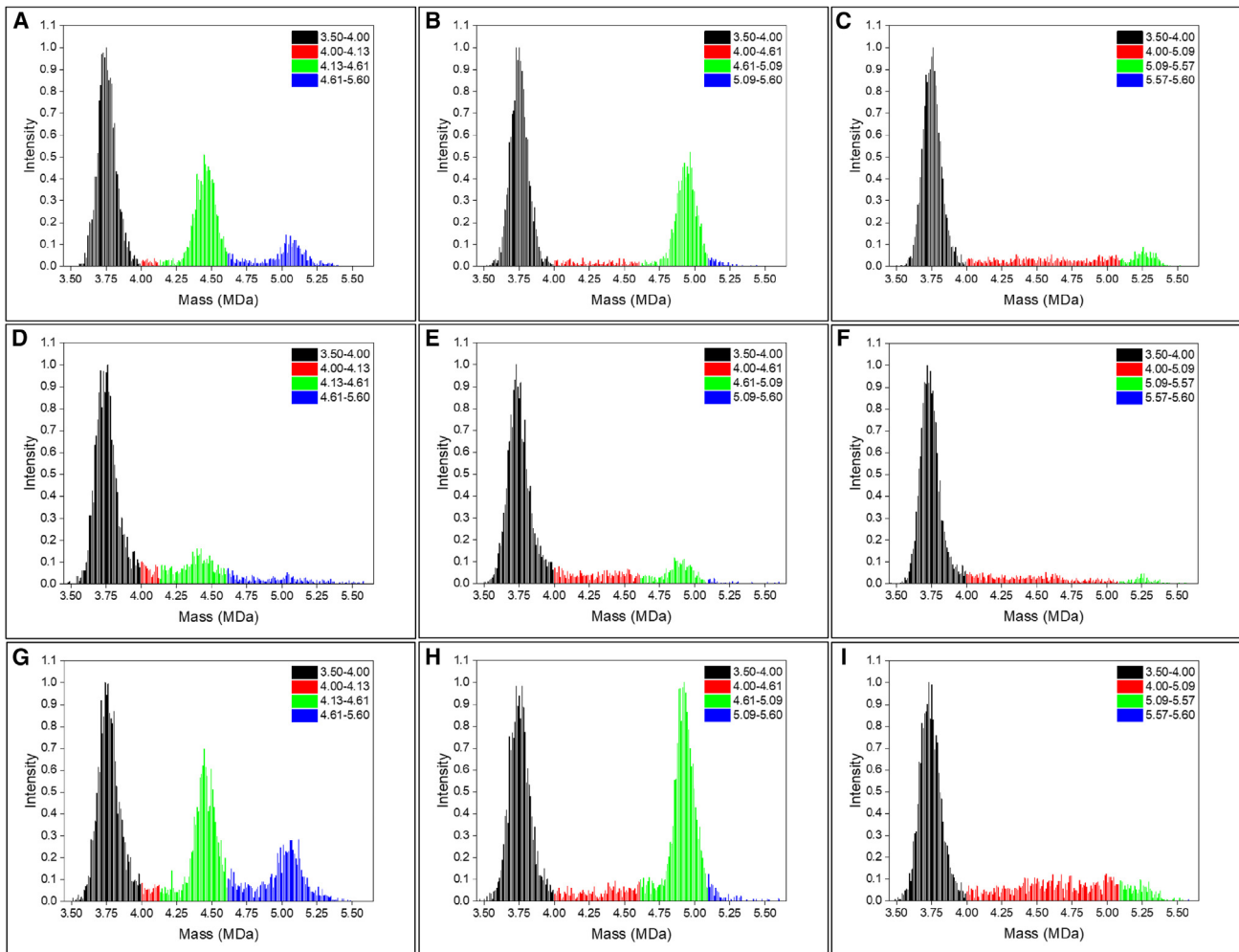


Figure 3. CD-MS mass histogram results for AAV2-GFP AEX chromatography full capsid peaks

(A) Transfection condition 1 AAV2-GFP 1.9 kb. (B) Transfection condition 1 AAV2-GFP 3.4 kb. (C) Transfection condition 1 AAV2-GFP 4.9 kb. (D) Transfection condition 2 AAV2-GFP 1.9 kb. (E) Transfection condition 2 AAV2-GFP 3.4 kb. (F) Transfection condition 2 AAV2-GFP 4.9 kb. (G) Transfection condition 3 AAV2-GFP 1.9 kb. (H) Transfection condition 3 AAV2-GFP 3.4 kb. (I) Transfection condition 3 AAV2-GFP 4.9 kb.

the AAV2 samples in this study were $\sim 10^{\circ}\text{C}$ higher, which may be due to the formulation containing surfactant. Previous studies examining AAV2 thermostability and genome ejection as a function of packaged genome length showed an inverse relationship such that larger genome sizes had less thermostability based on decreased genome ejection melting temperature, T_{m} .²⁹ This previous study used a formulation of only PBS buffer without any surfactants, which are typically added in protein formulations for improved thermostability. This previous study also defined the genome ejection melting temperature as the temperature at which 50% of the AAV genomes have been ejected from the capsids based on the fluorescence signal; thus, the genome ejection melting temperatures from this study could not be compared since in this study genome ejection melting temperature was defined as the maximum absorbance change (dA/dT) in the fluorescence intensity curve, resulting in two melting temperatures

(T_{m1} and T_{m2}). These data suggest that variable encapsidation in the AAV samples, as determined by CD-MS, did not significantly affect the genome ejection melting temperature (T_{m1}) under this sample formulation containing surfactant. The T_{m1} and T_{m2} observed in this study aligned with the kinetic model for genome uncoating proposed by Bernaud et al. showing a two-step single-stranded DNA (ssDNA) ejection behavior.³⁰ In the proposed model, the first step of genome ejection begins with a small length of the ssDNA exiting the intact capsid, with the full ejection being hindered by an energetic barrier. Once this second energy barrier is overcome as the temperature increases, then the complete ejection of the ssDNA occurs. This aligns with T_{m1} being the melting temperature of the ssDNA ejection of the intact capsid since it occurs $\sim 10^{\circ}\text{C}$ before the capsid completely disassembles, as observed by the T_{m2} and T_{agg} . These results suggest that AAV sample formulation can be

Table 2. Summarized CD-MS results of AAV2-GFP AEX full capsid peak samples

Transfection condition	Genome size, kb	Low MW, %	Empty capsid, %	Partial capsid, %	Full capsid, %	Copackaged capsid, %	High MW, %
1	1.9	0.2	55.5	1.0	30.4	11.2	1.7
	3.4	0.1	59.2	3.8	33.2	1.6	2.2
	4.9	0.0	75.8	15.4	6.5	0.0	2.3
2	1.9	2.6	65.8	3.5	14.3	6.5	7.4
	3.4	1.3	69.6	10.1	9.6	0.6	8.8
	4.9	1.2	74.8	12.0	2.1	0.0	9.8
3	1.9	2.9	34.1	1.5	23.1	15.6	22.9
	3.4	2.1	32.8	5.0	32.5	1.6	26.1
	4.9	2.3	50.3	20.5	5.0	0.0	21.9

CD-MS results of the AAV2-GFP samples showing the distribution of low-molecular-weight (MW) species, empty capsid, partial capsid, full capsid, copackaged capsid, and high-molecular-weight species.

optimized to increase AAV thermostability regardless of the extent of packaging.

MATERIALS AND METHODS

Plasmid constructs

A cytomegalovirus-GFP AAV genome plasmid (1.9 kb ITR-ITR length) was obtained from Sarepta Therapeutics (Burlington, MA). The parent genome plasmid was sent to ATUM (Newark, CA), which generated two plasmid clones each with an ~1.5 and 3.0 kb stuffer added inside the ITR-ITR region, respectively. The three plasmids were then sent to Aldevron (Fargo, ND) for plasmid production. The AAV2 rep/cap plasmid (pRep/Cap) used was pALD-AAV2 and the helper plasmid (pHelp) used was pALD-X80 (both by Aldevron). The ITR-ITR length of the plasmids are 1.9, 3.4, and 4.9 kb, respectively. The three genome of interest plasmids (pGOI) were analyzed by Aldevron and passed the quality control analysis for DNA homogeneity (predominantly supercoiled), identity, purity (based on A260/A280 absorbance ratio), residual host genomic

DNA, and restriction digestion matching the expected banding pattern.

Transfection reagent

The transfection reagent and cell culture medium used for preparing the transfection mix for all AAV2-GFP productions used procedures similar to those described in the literature.^{19–22,31}

Suspension adapted HEK293 cell culture

The first part of the study consisting of a DoE of 15 experiments for each GFP genome was performed in Corning 125 mL polycarbonate Erlenmeyer shake flasks (Corning Life Science, Tewksbury, MA) with a 30 mL working volume. The second part of the study, consisting of 4 experiments for each GFP genome, was performed in Corning 3-L polycarbonate Erlenmeyer shake flasks (Corning Life Science) with a 1 L working volume. The cell culture followed standard conditions of 37°C incubation with ≥ 80% relative humidity and 8% CO₂ on an orbital shaker platform. The VCD measurements were taken using the Vi-CELL XR Cell Viability Analyzer (Beckman Coulter, Brea, CA).

AAV production protocol

Suspension HEK293 cells were seeded into shake flasks and transfected once the target VCD at transfection was achieved within 24–48 h of cell growth. The transfection complex mix would be 5% of the total working volume of the cell culture and would be prepared by first adding the appropriate quantity of the three plasmids into the medium, mixing the solution, and then adding the appropriate quantity of transfection reagent; briefly vortexing the solution; and then incubating the transfection mix at room temperature for 30 min at rest. The transfection mix would then be added to the cell culture while shaking the flask. The cell culture would be harvested 72 h post-transfection and would be lysed by adding a chemical lysing solution with incubation for 2 h and then spun down using a centrifuge at 4,500 rpm for 2 min. The supernatant would be sampled and the cell pellet discarded. The mass quantity of each plasmid added was calculated based on the plasmid molar ratios of the experiment, the

Table 3. Summarized full capsid ratio results from orthogonal methods for AAV2-GFP AEX full capsid peak samples

Transfection condition	Genome size, kb	vg/cp, %	UV/DLS, %	CD-MS, %
1	1.9	11.57	27.04	30.40
	3.4	12.28	22.86	33.20
	4.9	3.76	5.49	6.50
2	1.9	5.69	12.88	14.30
	3.4	6.15	8.61	9.60
	4.9	1.64	2.87	2.10
3	1.9	10.12	22.60	23.10
	3.4	9.34	16.35	32.50
	4.9	1.35	4.05	5.00

The full capsid ratio (%) results for each AAV2-GFP AEX full capsid peak sample by vg/cp, UV/DLS, and CD-MS (%).

Table 4. The CE-SDS-LIF capsid purity results for the AAV2-GFP AEX full capsid peak samples

Transfection condition	Genome size, kb	VP1 area, %	VP2 area, %	VP3 area, %	Full capsid purity, %
1	1.9	15	13	68	96.1
	3.4	16	14	67	96.6
	4.9	13	13	71	96.3
2	1.9	12	11	71	93.9
	3.4	13	10	70	92.6
	4.9	14	10	71	95.5
3	1.9	15	15	65	94.4
	3.4	12	13	68	92.5
	4.9	12	13	66	91.1

The area under the curve of the electropherogram of the VP1, VP2, and VP3 peaks were added and the remaining low molecular peaks considered degraded VP impurities.

molecular weight of each plasmid, the DNA concentration ($\mu\text{g DNA}/\text{E}+06$ cells), and the VCD. The mass quantity of transfection reagent was calculated based on the mass ratio of PEI:DNA ($\mu\text{g}/\mu\text{g}$) and the total mass quantity of DNA being added for the transfection condition. This AAV production procedure was similar to those described in the literature.^{19–22,31}

Viral genome titer quantitation

The vg titer quantitation of centrifuged AAV cell culture supernatant and affinity capture chromatography purified AAV samples was tested by performing digital droplet PCR (ddPCR) following the BIO-RAD Bulletin 7407 AAV ddPCR protocol and previously described methods.³² The following probes and primers were used: GFP probe sequence, 5'-HEX-CC TGA GCA A-ZEN-A GAC CCC AAC GAG AA-3'-IABkFQ; GFP forward primer, 5'-GACAACCAC-TACCTGAGCAC-3'; and GFP reverse primer, 5'-CAGGAC-CATGTGATCGCG-3'. Negative controls were performed using buffer blanks.

Capsid titer quantitation

The cp titer quantitation of affinity capture chromatography-purified AAV samples was performed using the Sartorius Octet system using biolayer interferometry following the Sartorius Octet AAV2 Quantitation Application Note.³³ The standard curve was performed using the AAV2 reference standard by the American Type Culture Collection (catalog no. VR-1616). Negative controls were performed using buffer blanks. Cell culture supernatant samples had matrix effects that did not allow for capsid octet quantitation.

Affinity capture chromatography purified AAV2-GFP

AAV2-GFP was produced using suspension-adapted HEK293 cells in a 3 L shake flask with 1 L working volume for each GFP genome size (1.9, 3.4, and 4.9 kb) for 3 separate transfection conditions. The frozen cell culture harvest was thawed, 0.45- μm bottle top filtered using a vacuum, and then loaded onto a 5 mL AAVX

Pre-Packed column at a flow rate of 5 mL/min (1-min residence time). All of the affinity capture chromatography experiments used POROS GoPure AAVX Pre-Packed 5-mL columns (Thermo Fisher Scientific, Bedford, MA). The affinity capture chromatography experiments were performed using an AKTA Pure 25 system (Cytiva, Marlborough, MA) connected to a fraction collector. The affinity capture chromatography step would first be a 5 column volume (CV) wash with equilibration buffer, followed by loading, a 5 CV wash with equilibration buffer, and then elution with 5 CV of elution buffer similar to those described in the literature.⁷ The eluate would then be titrated to pH 8 and sampled.

AEX

AEX chromatography column, buffers, and method were similar to those described in the literature.^{3,5–7} All of the experiments were performed using an AKTA Pure 25 system (Cytiva) connected to a fraction collector. The affinity-purified AAV2-GFP samples were prepared and loaded onto the AEX column at a capsid load ranging from $4.6\text{E}+13$ to $4.6\text{E}+14$ cp/mL. The column was then chased with 5 CV of equilibration buffer. The column would then be washed with a linear gradient of equilibration buffer and salt elution buffer for full to empty (F/E) AAV capsid separation. The column eluate was collected in 1 mL column fractions using a 96 deep well plate and pooled based on the UV A260/A280 ratios of the chromatogram, with the eluted empty capsids having an absorbance peak with A260/A280 < 1 and the full-genome-containing capsids having an absorbance peak with A260/A280 > 1. All of the chromatography steps were performed at 5 CV/min in the downflow direction at ambient temperature. The conductivity values and elution times taken of the peaks from each AEX experiment are the respective values at the A280 peak maxima value.

UV/DLS AAV full/empty ratio quantitation

The Stunner instrument by Unchained Labs (Brighton, MA) quantifies the F/E ratio of AAV samples by measuring UV-visible spectroscopy, DLS, and user inputs of the expected packaged genome length and amino acid sequence of the specific AAV serotype of the sample to calculate the vg titer, cp titer, and F/E ratio using its AAV Quant software. Since the lower limits of detection (LLOD) are $1\text{E}+12$ vg/mL and $2\text{E}+12$ cp/mL according to Yang et al., the AAV2-GFP samples generated were concentrated using Millipore Amicon 50 kDa molecular weight cutoff spin filters (MilliporeSigma, Bedford, MA) to titers above the Stunner LLOD to quantify the F/E ratio.³⁴ Samples were then also submitted for CD-MS to Megadalton Solutions for analysis.

CD-MS

All of the samples were stored at -80°C before analysis. AAV samples were thawed on ice before buffer exchange into 200 mM ammonium acetate (Invitrogen, AM9070G) using desalting spin columns (Bio-Rad, 7326228). The exchanged samples were then stored at 4°C in a commercial Triversa Nanomate (Advion, A Chip) electrospray source. Samples were measured by a research-grade CD-MS

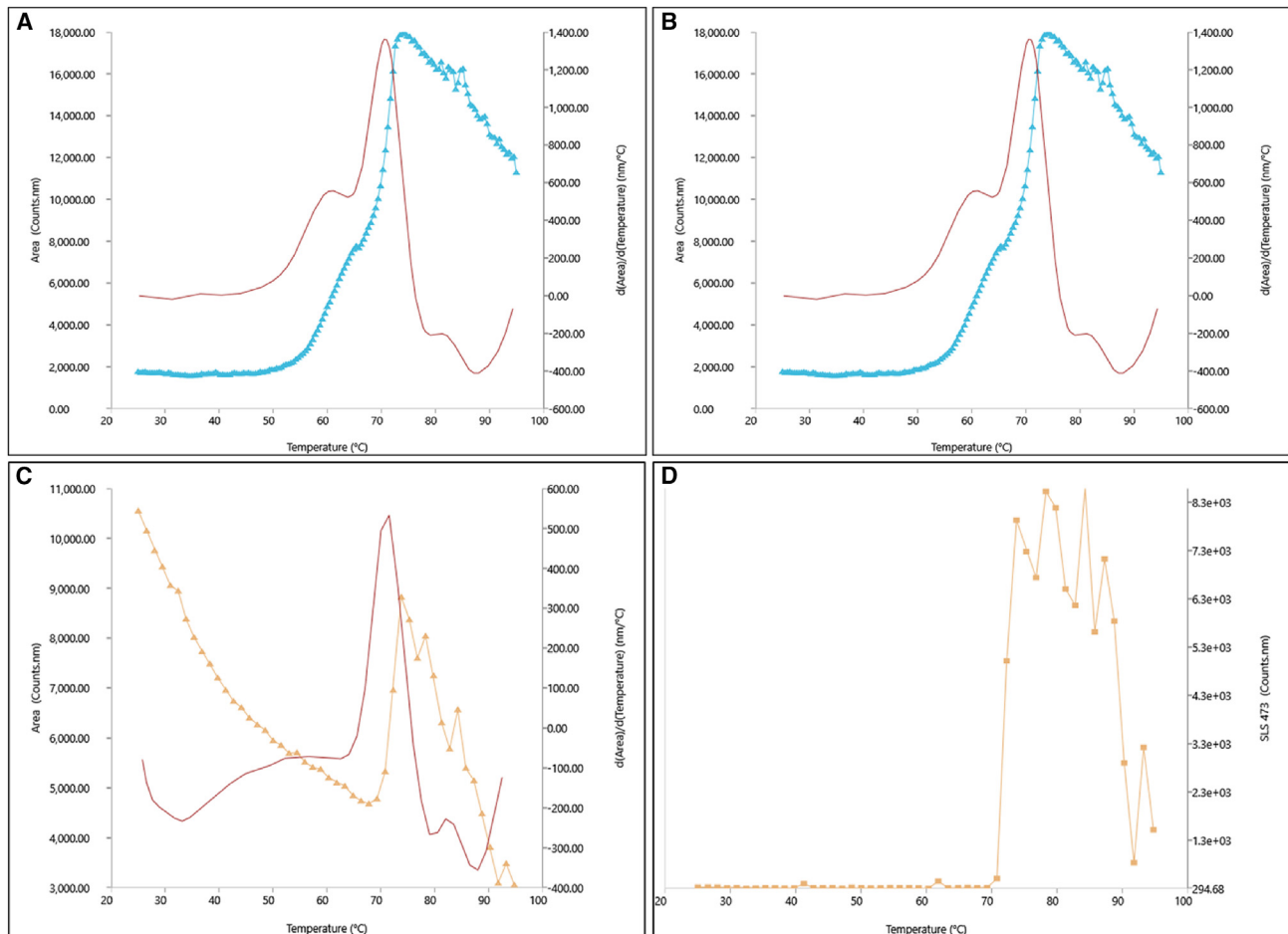


Figure 4. Genome ejection melting curves and SLS 473 intensity curve for AEX full and empty capsid peak samples

(A) The genome ejection melting curve (blue) based on fluorescent intensity of SYBR Gold bound to DNA for condition 1 AAV2-GFP AEX full capsid peak 1.9 kb sample. The differential (red) is graphed as well to show the maxima, which would be the melting temperature, T_m . $T_{m1, avg.} = 59.83^\circ\text{C}$ and $T_{m2, avg.} = 69.53^\circ\text{C}$. (B) The SLS 473 intensity curve (blue) showing aggregation of the condition 1 AAV2-GFP AEX full capsid peak 1.9 kb sample. $T_{agg., avg.} = 71.78^\circ\text{C}$. (C) The genome ejection melting curve (yellow) based on fluorescent intensity of SYBR Gold bound to DNA for condition 1 AAV2-GFP AEX empty capsid peak 1.9 kb sample. The differential (red) is graphed as well to show the maxima, which would be the melting temperature, T_m . $T_{m, avg.} = 71.93^\circ\text{C}$. (D) The SLS473 intensity curve (yellow) showing aggregation of the condition 1 AAV2-GFP AEX empty capsid peak 1.9-kb sample. $T_{agg., avg.} = 69.99^\circ\text{C}$.

instrument with components described previously.^{35–37} The mass of each AAV ion is determined by simultaneous measurement of m/z and z to allow for a direct calculation of mass. All of the experiments were measured with an ion energy of 100 eV/ z and a trapping time of 100 ms to give a charge uncertainty of $\sim 1e$. Each CD-MS mass spectrum was collected to have over 5,000 AAV capsid ions. Data were interpreted by binning single ion measurements into histograms with 10,000-Da bins. All of the masses were assigned with Gaussian peak fits in OriginPro.

Capsid protein purity quantitation

AAV capsid protein quantitation was performed using a CE-SDS-LIF method with the PA800 Plus Biologics Analysis System by SCIEX following the SCIEX Technical Note: Purity Analysis of AAV Capsid Proteins using CE-LIF Technology.

DoE study design, statistical analysis, and modeling

All of the statistical analyses were performed using JMP version 14.0.0. Experimental results were statistically analyzed by ANOVA and fitting the data to a standard least squares model and calculating the summary of fit and parameter estimates for significance with $p < 0.05$. The factors in the custom DoE generated in the small shake flask study were set discrete variables to keep the total number of small-scale experiments to 45 runs due to material constraints. Using a 6-factor response surface design DoE would require a minimum of 46 runs with a central composite design, which for each GFP genome would total 138 runs.

DSF for AAV thermostability

DSF experiments were performed using the UNcle instrument (Un-chained Labs) which is a multimodal thermostability platform with

3 detection methods consisting of full-spectrum fluorescence, SLS, and DLS to quickly profile viral thermostability using temperature control (15°C–95°C). The application note by Unchained Labs describes the method to study the thermostability of an AAV sample with a minimum vg titer of 5E+11 vg/mL using SYBR Gold dye-based fluorescence.²⁸

DATA AND CODE AVAILABILITY

All of the data needed to evaluate the conclusions in the paper are present in this paper and/or the supplemental information. For additional requests about the data, please reach out to the corresponding author, N.I.

SUPPLEMENTAL INFORMATION

Supplemental information can be found online at <https://doi.org/10.1016/j.omtm.2024.101188>.

ACKNOWLEDGMENTS

The authors thank Sarepta Therapeutics (Burlington, MA) for funding the project. The authors also thank Megadalton Solutions for collaborating on this project and performing CD-MS analysis on samples, and Alexandra Duffy and Anela Omerovic for performing the CE-SDS-LIF analysis on samples for capsid protein purity quantitation.

AUTHOR CONTRIBUTIONS

N.I. conceptualized the idea and developed the methodology under the guidance of C.W.L. N.I. performed the investigation and writing of the manuscript. B.E.D. performed the CD-MS testing, analysis, and writing of the manuscript.

DECLARATION OF INTERESTS

N.I. is a full-time employee at Sarepta Therapeutics, a company with interest in developing AAV technology, and B.E.D. is a full time employee at Megadalton Solutions, a company with interest in developing CD-MS technology. C.W.L. declares no competing interests.

REFERENCES

- U.S. Food and Drug Administration Cellular, Tissue, and Gene Therapies Advisory Committee Meeting #70 (2021). Toxicity Risks of Adeno-associated Virus (AAV) Vectors for Gene Therapy (GT) (Briefing Document).
- Segura, M.M., Kamen, A.A., and Garnier, A. (2011). Overview of Current Scalable Methods for Purification of Viral Vectors. *Methods Mol. Biol.* 737, 89–116.
- Dickerson, R., Argento, C., Pieracci, J., and Bakhshayeshi, M. (2021). Separating Empty and Full Recombinant Adeno-Associated Virus Particles Using Isocratic Anion Exchange Chromatography. *Biotech. J.* 16, e2000015.
- Venkatakrishnan, B., Yarbrough, J., Domsic, J., Bennett, A., Bothner, B., Kozyreva, O.G., Samulski, R.J., Muzyczka, N., McKenna, R., and Agbandje-McKenna, M. (2013). Structure and Dynamics of Adeno-Associated Virus Serotype 1 VP1-Unique N-Terminal Domain and Its Role in Capsid Trafficking. *J. Virol.* 87, 4974–4984.
- Wang, C., Mulagapati, S.H.R., Chen, Z., Du, J., Zhao, X., Xi, G., Chen, L., Linke, T., Gao, C., Schmelzer, A.E., and Liu, D. (2019). Developing an Anion Exchange Chromatography Assay for Determining Empty and Full Capsid Contents in AAV6.2. *Mol. Ther. Methods Clin. Dev.* 15, 257–263.
- Khatwani, S.L., Pavlova, A., and Pirot, Z. (2021). Anion-exchange HPLC assay for separation and quantification of empty and full capsids in multiple adeno-associated virus serotypes. *Mol. Ther. Methods Clin. Dev.* 21, 548–558.
- Joshi, P.R.H., Bernier, A., Moço, P.D., Schrag, J., Chahal, P.S., and Kamen, A. (2021). Development of a scalable and robust AEX method for enriched rAAV preparations in genome-containing VCs of serotypes 5, 6, 8, and 9. *Mol. Ther. Methods Clin. Dev.* 21, 341–356.
- Wörner, T.P., Bennett, A., Habka, S., Snijder, J., Friese, O., Powers, T., Agbandje-McKenna, M., and Heck, A.J.R. (2021). Adeno-associated virus capsid assembly is divergent and stochastic. *Nat. Commun.* 12, 1642.
- Mary, B., Maurya, S., Arumugam, S., Kumar, V., and Jayandharan, G.R. (2019). Post-translational modifications in capsid proteins of recombinant adeno-associated virus (AAV) 1-rh10 serotypes. *FEBS J.* 286, 4964–4981.
- Giles, A.R., Sims, J.J., Turner, K.B., Govindasamy, L., Alvira, M.R., Lock, M., and Wilson, J.M. (2018). Deamidation of Amino Acids on the Surface of Adeno-Associated Virus Capsids Leads to Charge Heterogeneity and Altered Vector Function. *Mol. Ther.* 26, 2848–2862.
- Li, T., Gao, T., Chen, H., Pekker, P., Menyhart, A., and Guttman, A. (2020). Rapid Determination of Full and Empty Adeno-Associated Virus Capsid Ratio by Capillary Isoelectric Focusing. *Curr. Mol. Med.* 20, 814–820.
- Wu, J., and Heger, C. (2022). Establishment of a platform imaged capillary isoelectric focusing (icIEF) characterization method for adeno-associated virus (AAV) capsid proteins. *Elsev. Gre. Ana. Chem.* 3, 100027.
- Dong, J.Y., Fan, P.D., and Frizzell, R.A. (1996). Quantitative Analysis of the Packaging Capacity of Recombinant Adeno-Associated Virus. *Hum. Gene Ther.* 7, 2101–2112.
- Hermonat, P.L., Quirk, J.G., Bishop, B.M., and Han, L. (1997). The Packaging Capacity of Adeno-Associated Virus (AAV) and the Potential for Wild-Type-Plus AAV Gene Therapy Vectors. *FEBS J.* 407, 78–84.
- Grieger, J.C., and Samulski, R.J. (2005). Packaging Capacity of Adeno-Associated Virus Serotypes: Impact of Larger Genomes on Infectivity and Postentry Steps. *J. Virol.* 79, 9933–9944.
- Tai, P.W.L., Xie, J., Fong, K., Seetin, M., Heiner, C., Su, Q., Weiland, M., Wilmot, D., Zapp, M.L., and Gao, G. (2018). Adeno-associated Virus Genome Population Sequencing Achieves Full Vector Genome Resolution and Reveals Human-Vector Chimeras. *Mol. Ther. Methods Clin. Dev.* 9, 130–141.
- Wu, Z., Yang, H., and Colosi, P. (2010). Effect of Genome Size on AAV Vector Packaging. *Mol. Ther.* 18, 80–86.
- Meade, O., Clark, J., McCutchen, M., and Kerwin, J. (2021). Exploring the design space of AAV transient-transfection in suspension cell lines. *Methods Enzymol.* 660, 341–360.
- Durocher, Y., Pham, P.L., St-Laurent, G., Jacob, D., Cass, B., Chahal, P., Lau, C.J., Nalbantoglu, J., and Kamen, A. (2007). Scalable serum-free production of recombinant adeno-associated virus type 2 by transfection of 293 suspension cells. *J. Virol Methods* 144, 32–40.
- Huang, X., Hartley, A.V., Yin, Y., Herskowitz, J.H., Lah, J.J., and Ressler, K.J. (2013). AAV2 production with optimized N/P ratio and PEI-mediated transfection results in low toxicity and high titer for in vitro and in vivo applications. *J. Virol Methods* 193, 270–277.
- Chahal, P.S., Schulze, E., Tran, R., Montes, J., and Kamen, A.A. (2014). Production of adeno-associated virus (AAV) serotypes by transient transfection of HEK293 cell suspension cultures for gene delivery. *J. Virol.* 196, 163–173.
- Grieger, J.C., Soltys, S.M., and Samulski, R.J. (2016). Production of Recombinant Adeno-associated Virus Vectors Using Suspension HEK293 Cells and Continuous Harvest of Vector From the Culture Media for GMP FIX and FLT1 Clinical Vector. *Mol. Ther.* 24, 287–297.
- Werle, A.K., Powers, T.W., Zobel, J.F., Wappelhorst, C.N., Jarrold, M.F., Lykтей, N.A., Sloan, C.D.K., Wolf, A.J., Adams-Hall, S., Baldus, P., and Runnels, H.A. (2021). Comparison of analytical techniques to quantitate the capsid content of adeno-associated viral vectors. *Mol. Ther. Methods Clin. Dev.* 23, 254–262.
- Maruno, T., Usami, K., Ishii, K., Torisu, T., and Uchiyama, S. (2021). Comprehensive Size Distribution and Composition Analysis of Adeno-Associated Virus Vector

- by Multiwavelength Sedimentation Velocity Analytical Ultracentrifugation. *J. Pharmaceut. Sci.* *110*, 3375–3384.
25. Pacouret, S., Bouzelha, M., Shelke, R., Andres-Mateos, E., Xiao, R., Maurer, A., Mevel, M., Turunen, H., Barungi, T., Penaud-Budloo, M., et al. (2017). AAV-ID A Rapid and Robust Assay for Batch-to-Batch Consistency Evaluation of AAV Preparations. *Mol. Ther.* *25*, 1375–1386.
 26. Rayaprolu, V., Kruse, S., Kant, R., Venkatakrishnan, B., Movahed, N., Brooke, D., Lins, B., Bennett, A., Potter, T., McKenna, R., et al. (2013). Comparative Analysis of Adeno-Associated Virus Capsid Stability and Dynamics. *J. Virol.* *87*, 13150–13160.
 27. Bennett, A., Patel, S., Mietzsch, M., Jose, A., Lins-Austin, B., Yu, J.C., Bothner, B., McKenna, R., and Agbandje-McKenna, M. (2017). Thermal Stability as a Determinant of AAV Serotype Identity. *Mol. Ther. Methods Clin. Dev.* *6*, 171–182.
 28. UNCHAINED LABS (2020). DNA Leaks before Capsids Pop: AAV Thermal Stability on Uncle, Application Note Rev A.
 29. Horowitz, E.D., Rahman, K.S., Bower, B.D., Dismuke, D.J., Falvo, M.R., Griffith, J.D., Harvey, S.C., and Asokan, A. (2013). Biophysical and Ultrastructural Characterization of Adeno-Associated Virus Capsid Uncoating and Genome Release. *J. Virol.* *87*, 2994–3002.
 30. Bernaud, J., Rossi, A., Fis, A., Gardette, L., Aillot, L., Büning, H., Castelnovo, M., Salvetti, A., and Faivre-Moskalenko, C. (2018). Characterization of AAV vector particle stability at the single-capsid level. *J. Biol. Phys.* *44*, 181–194.
 31. Zhao, H., Lee, K.J., Daris, M., Lin, Y., Wolfe, T., Sheng, J., Plewa, C., Wang, S., and Meisen, W.H. (2020). Creation of a High-Yield AAV Vector Production Platform in Suspension Cells Using a Design-of-Experiment Approach. *Mol. Ther. Methods Clin. Dev.* *18*, 312–320.
 32. Dobnik, D., Kogovšek, P., Jakomin, T., Košir, N., Tušek Žnidarič, M., Leskovec, M., Kaminsky, S.M., Mostrom, J., Lee, H., and Ravnikar, M. (2019). Accurate Quantification and Characterization of Adeno-Associated Viral Vectors. *Front. Microbiol.* *10*, 1570.
 33. Sartorius, and Li, H. (2021). Rapid, Automated, At-Line AAV2 Virus Quantitation Advances Bioprocessing in Gene Therapy. Sartorius Application Note.
 34. Yang, Q.E., Walton, R.W., Kudrolli, T., Denys, N., Lance, K., and Chang, A. (2022). Rapid Quality Control Assessment of Adeno-Associated Virus Vectors Via Stunner. *GEN Biotechnol* *1*, 300–310.
 35. Contino, N.C., and Jarrold, M.F. (2013). Charge detection mass spectrometry for single ions with a limit of detection of 30 charges. *Int. J. Mass Spectrom.* *345–347*, 153–159.
 36. Draper, B.E., Anthony, S.N., and Jarrold, M.F. (2018). The FUNPET—a New Hybrid Ion Funnel-Ion Carpet Atmospheric Pressure Interface for the Simultaneous Transmission of a Broad Mass Range. *J. Am. Soc. Mass Spectrom.* *29*, 2160–2172.
 37. Draper, B.E., and Jarrold, M.F. (2019). Real-Time Analysis and Signal Optimization for Charge Detection Mass Spectrometry. *J. Am. Soc. Mass Spectrom.* *30*, 898–904.